

Bandgap Energy of Cu₂ZnSnS₄ Quantum Well with Modified Deformed Hylleraas Potential in the Presence of Magnetic Field

Roli E. Oloko,* Ephraim O. Chukwuocha and Ndem A. Ikot

Department of Physics, University of Port Harcourt, Choba, Port Harcourt, Rivers State, Nigeria

*rolioloko@uniport.edu.ng

Abstract

The behaviour of Cu₂ZnSnS₄ quantum well confined in the modified deformed Hylleraas potential have been examined within the framework of the Nikiforov-Uvarov method of solving the radial part of the Schrodinger wave equation. The bandgap energies E_{nl} are numerically calculated with an applied magnetic field B(T) in order to show their influence on the bandgap energy E_{nl} . Our results show that the bandgap energy E_{nl} is significantly dependent on the applied magnetic field B(T) as well as parameters of the confining potential.

Keywords: magnetic field, modified deformed Hylleraas potential, Nikiforov-Uvarov method, quantum well

Introduction

In the last few decades, there has been serious energy crisis and environmental pollution, which are of great concern. In dealing with this crisis, research on renewable sources of energy such as solar energy that are environmentally clean, abundant and readily available was carried out (Chen *et al.*, 2013; Boda, 2013; Uplane *et al.*, 2000), obtained high conversion efficiency of solar energy, ideal solar energy absorbers, which are usually semiconductor materials having a direct bandgap between 1.30–1.50 eV are required (Liu *et al.*, 2015; Panahi *et al.*, 2013; Aytekin *et al.*, 2012; Allouche *et al.*, 2010).

Advances in fabrication techniques have made it possible through Molecular Beam Epitaxy (MBE) to combine elements across groups and periods in the periodic table following a combination ratio to form binary, ternary, quaternary and pentanary compounds and also using modern technological techniques to predict the physical properties of these compounds (Karanslan *et al.*, 2016; Wang *et al.*, 2013; Liu *et al.*, 2015). Presently, cadmium telluride (CdTe) and copper indium gallium selenide (Cu(In,Ga)Se₂(CIGS) have reached commercialisation stages as buffer layers in thin film solar cells (TFSC) but concerns with price and availability of indium in CIGS and tellurium in CdTe as well as the toxicity of cadmium have motivated the search for alternative thin film solar cell materials. Copper zinc tin sulphide (Cu₂ZnSnS₄ or CZTS) has emerged as a potential replacement for CIGS and CdTe as TFSC

Materials and Methods

A system comprising of a carrier moving in a Cu₂ZnSnS₄ quantum well modified deformed Hylleraas confining potential was considered and

placed in an external magnetic field B. The corresponding Hamiltonian may be written as

$$H = \left[\frac{1}{2} m^* \left(P - \frac{q}{c} A \right)^2 + V(r) \right] \Psi(r) \quad (1)$$

$$H \Psi(r) = E \Psi(r) \quad (2)$$

$$\left[\frac{1}{2} m^* \left(P - \frac{q}{c} A \right)^2 + V(r) \right] \Psi(r) = E \Psi(r) \quad (3)$$

$$\left[\frac{-\hbar^2 \nabla^2}{2m^*} - \frac{qB}{2m^*} L \frac{q^2 B^2 r^2}{8m^*} + V(r) \right] \Psi(r) = E \Psi(r) \quad (4)$$

$$\omega_c = \frac{qB}{m^*} \quad (5)$$

ω_c is the cyclotron frequency

$$\left[\frac{-\hbar^2 \nabla^2}{2m^*} - \frac{1}{2} \omega_c r L + \frac{1}{8} + m^* \omega_c^2 r^2 + V(r) \right] \varphi(r) = E \varphi(r) \quad (6)$$

Where ∇^2 is the 2-D and L is the angular momentum operator $\frac{\hbar}{d\vartheta^1}$ with eigen value $\hbar m$ in the polar coordinates (r, ϑ) using the following eigen function

$$\varphi(r) = \frac{e^{im\vartheta} R(r)}{\sqrt{2\pi} \sqrt{r}} \quad (7)$$

According to the effective mass theory (EMT), the radial S.E. for an excited electron in a spherical QD given by

$$\frac{d^2 R}{dr^2} + \left[\frac{2m^*}{\hbar^2} [E - V(r)] - \frac{1}{2} \frac{\omega_c \hbar m^*}{r} - \frac{(m^2 - 1/4) \hbar^2}{2m^* r^2} - \frac{1}{8} \frac{M^* \omega_c^2 r/2}{r/2} \right] R(r) = 0 \quad (8)$$

$$\frac{d^2 R}{dr^2} + \left[\frac{2m^*}{\hbar^2} [E - V(r)] - \frac{1}{2} \frac{\omega_c \hbar m^*}{r} - \frac{1}{8} m^* \omega_c^2 - \frac{\ell(\ell+1)}{r^2} \right] R(r) = 0 \quad (9)$$

Introducing the deformed Hylleraas potential given by Hassanabadi *et al.* (2017), Ikot *et al.* (2013) and Pena *et al.* (2015).

$$V_{(r)} = \frac{V_0}{b} \left(\frac{a-e^{-ar}}{1-e^{-ar}} \right) - \frac{V_1 e^{-ar}}{1-e^{-ar}} + \frac{V_2 e^{-2ar}}{(1-e^{-ar})^2} \quad (10)$$

Equation (10) in equation (9) gives

$$\frac{d^2 R}{dr^2} + \left[\frac{2m^*}{\hbar^2} \left[E - \frac{V_0}{b} \left(\frac{a-e^{-ar}}{1-e^{-ar}} \right) - \frac{V_1 e^{-ar}}{1-e^{-ar}} + \frac{V_2 e^{-2ar}}{(1-e^{-ar})^2} \right] - \frac{1}{2} \frac{\omega_c \hbar m^*}{r} - \frac{1}{8} m^* \omega_c^2 - \frac{\ell(\ell+1)}{r^2} \right] R_{(r)=0} \quad (11)$$

Equation (11) cannot have a direct solution because of the presence of the centrifugal term $\frac{1}{r^2}$, therefore an approximation term is introduced in the form (Greene and Aldrich, 1976).

$$\frac{1}{r^2} = \frac{4e^2 e^{-2ar}}{(1-e^{-ar})^2}; \quad \frac{1}{r} = \frac{2\alpha r e^{-ar}}{1-e^{-ar}} \quad (12)$$

Substituting equation (12) into equation (11)

$$\frac{d^2 R}{dr^2} + \left[\frac{2m^*}{\hbar^2} \left[E - \frac{V_0}{b} \left(\frac{a-e^{-ar}}{1-e^{-ar}} \right) - \frac{V_1 e^{-ar}}{1-e^{-ar}} + \frac{V_2 e^{-2ar}}{(1-e^{-ar})^2} \right] - \frac{1}{2} \frac{\omega_c \hbar m^*}{r} - \frac{1}{8} m^* \omega_c^2 - \frac{\ell(\ell+1)}{r^2} \cdot \frac{4e^2 e^{-2ar}}{(1-e^{-ar})^2} \right] R_{(r)=0} \quad (13)$$

$$- \alpha e^{-ar} \frac{d^2 R}{ds^2} + \alpha^2 e^{-ar} \frac{dR}{ds} + \left[\frac{2m^*}{\hbar^2} \left[E - \frac{V_0}{b} \left(\frac{a-e^{-ar}}{1-e^{-ar}} \right) - \frac{V_1 e^{-ar}}{1-e^{-ar}} + \frac{V_2 e^{-2ar}}{(1-e^{-ar})^2} \right] - \frac{1}{2} \frac{\omega_c \hbar m^*}{r} \cdot \frac{2\alpha e^{-ar}}{(1-e^{-ar})^2} - \frac{1}{8} m^* \omega_c^2 - \ell(\ell+1) \cdot \frac{4e^2 e^{-2ar}}{(1-e^{-ar})^2} \right] R_{(r)=0} \quad (14)$$

Using coordinate transformation of the form $R \rightarrow S$ by setting $S = e^{-ar}; S^2 = e^{-2ar}$

Replace all exponential terms in equation (14) with S

$$\alpha^2 S^2 \frac{d^2 R}{ds^2} + \alpha^2 S \frac{dR}{ds} + \left[\frac{2m^*}{\hbar^2} \left[E - \frac{V_0}{b} \left(\frac{a-S^2}{1-S} \right) + \frac{V_1 S}{1-S} - \frac{V_2 S^2}{(1-S)^2} \right] - \omega_c \hbar m^* \frac{S}{1-S} - \frac{1}{8} m^* \omega_c^2 - \ell(\ell+1) \cdot \frac{4e^2 S^2}{(1-S)^2} \right] R_{(r)=0} \quad (15)$$

Divide equation (15) by $\alpha^2 S^2$

$$\frac{d^2 R}{ds^2} + \frac{1}{S} \frac{dR}{ds} + \frac{1}{\alpha^2 S^2} + \left[\frac{2m^* E}{\hbar^2} - \frac{2m^* V_0}{\hbar^2 b} \left(\frac{a-S^2}{1-S} \right) + \frac{2m^* V_1 S}{\hbar^2 (1-S)} - \frac{2m^* V_2 S^2}{\hbar^2 (1-S)^2} - \frac{\omega_c \hbar m^* S}{1-S} - \frac{1}{8} m^* \omega_c^2 - 4\ell(\ell+1) \cdot \frac{\alpha^2 S^2}{(1-S)^2} \right] R_{(r)=0} \quad (16)$$

$$\frac{d^2 R}{ds^2} + \frac{1}{S} \frac{dR}{ds} + \left[\frac{2m^* E}{\hbar^2 \alpha^2} - \frac{2m^* V_0}{\hbar^2 \alpha^2 b} \left(\frac{a-S}{1-S} \right) + \frac{2m^* V_1 S}{\hbar^2 \alpha^2 S^2 (1-S)} - \frac{2m^* V_2 S^2}{\hbar^2 \alpha^2 S^2 (1-S)^2} - \frac{\omega_c \hbar m^* S}{\alpha^2 S^2 (1-S)} - \frac{1}{8} \frac{m^* \omega_c^2}{\alpha^2 S^2} - \frac{4\ell(\ell+1) S^2}{S^2 (1-S)^2} \right] R_{(r)=0} \quad (17)$$

$$\frac{d^2 R}{ds^2} + \frac{1}{S} \frac{dR}{ds} + \frac{1}{S^2 (1-S)^2} + \left[\frac{2m^* E (1-S)^2}{\hbar^2 \alpha^2} - \frac{2m^* V_0 (a-S^2)(1-S)}{\hbar^2 \alpha^2 b} + \frac{2m^* V_1 S (1-S)}{\hbar^2 \alpha^2} - \frac{2m^* V_2 S^2}{\alpha^2} - \frac{\omega_c S (1-S) \hbar m^*}{1-S} - \frac{m^* \omega_c^2 (1-S)^2}{8\alpha^2} - 4\ell(\ell+1) S^2 \right] R_{(r)=0} \quad (18)$$

$$\frac{d^2 R}{ds^2} + \frac{1}{S} \frac{dR}{ds} + \frac{1}{S^2 (1-S)^2} + \left[\frac{2m^* E (1-2S+S^2)}{\hbar^2 \alpha^2} - \frac{2m^* V_0 (a-2S+S^2)(S-S^2)}{\hbar^2 \alpha^2 b} + \frac{2m^* V_1 (S-S^2)}{\hbar^2 \alpha^2} - \frac{2m^* V_2 S^2}{\hbar^2 \alpha^2} - \frac{\omega_c \hbar m^* (1-S)}{\alpha^2} - \frac{m^* \omega_c^2 (1-2S+S^2)}{8\alpha^2} - 4\ell(\ell+1) S^2 \right] R_{(r)=0} \quad (19)$$

$$\frac{d^2 R}{ds^2} + \frac{1}{S} \frac{dR}{ds} + \frac{1}{S^2 (1-S)^2} \left[-K^2 S^2 + \left(-\frac{2m^* V_0}{\hbar^2 \alpha^2 b} - \frac{2m^* V_1}{\hbar^2 \alpha^2} + \frac{\omega_c \hbar m^* 8}{\alpha^2} \right) S^2 - \left(\frac{2m^* V_2}{\hbar^2 \alpha^2} + \frac{m^* \omega_c^2}{8\alpha^2} 4\ell(\ell+1) \right) S^2 - \left(\frac{m^* \omega_c^2}{8\alpha^2} \right) S^2 + 2K^2 S + \left(\frac{2m^* V_0 a}{\hbar^2 \alpha^2 b} \right) S + \left(\frac{2m^* V_0}{\hbar^2 \alpha^2} + \frac{2m^* V_1}{\hbar^2 \alpha^2} - \frac{\omega_c \hbar m^*}{\alpha^2} \right) S + \left(\frac{m^* \omega_c^2}{4^2} \right) S - K^2 - \left(\frac{-2m^* V_0 a}{\hbar^2 \alpha^2 b} \right) - \left(\frac{m^* \omega_c^2}{8\alpha^2} \right) \right] R_{(r)=0} \quad (20)$$

$$\text{where } -K^2 = \frac{2m^* E}{\hbar^2 \alpha^2} \quad (21)$$

$$\left. \begin{aligned} \text{Let } N &= \frac{2m^* V_0}{\hbar^2 \alpha^2} + \frac{2m^* V_1}{\hbar^2 \alpha^2} - \frac{\omega_c \hbar m^*}{\alpha^2} \\ Z &= \frac{2m^* V_2}{\hbar^2 \alpha^2} + 4\ell(\ell+1) \\ H &= \frac{2m^* V_0 a}{\hbar^2 \alpha^2 b} \\ Q &= \frac{m^* \omega_c^2}{8^2}, 2Q = \frac{m^* \omega_c^2}{4^2} \end{aligned} \right\} \quad (22)$$

$$\frac{d^2 R}{ds^2} + \frac{1(1-S)}{S(1-S)} + \frac{1}{S^2 (1-S)^2} [-K^2 S^2 - NS^2 - ZS^2 - QS^2 + 2K^2 S + HS + NS + 2QS - K^2 - H - Q] R_{(r)=0} \quad (23)$$

$$\frac{d^2 R}{ds^2} + \frac{1}{S} \frac{dR}{ds} + \frac{1}{S^2 (1-S)^2} [-K^2 + N + Z + Q] S^2 + (2K^2 + H + N + 2Q) S - (K^2 + H + Q) R_{(r)=0} \quad (24)$$

Comparing equation (24) with the standard NU-equation

$$\varphi^{11} + \frac{\alpha_1 - \alpha_2 S}{S((1 - \alpha_3 S))} \varphi^1 + \frac{1}{S^2 ((1 - \alpha_3 S)^2)} [-\varepsilon_1 S^2 + \varepsilon_2 S + \varepsilon_3] \varphi = 0 \quad (25)$$

$$\begin{aligned}
 \alpha_1 &= 1, \alpha_2 = 1, \alpha_3 = 1, \alpha_4 = \frac{1-\alpha_1}{2} = 0 \\
 \alpha_5 &= \frac{\alpha_2 - 2\alpha_3}{2} = \frac{1-2}{2} = -\frac{1}{2} \\
 \epsilon_{d1} &= K^2 + N + Z + Q, \epsilon_{d2} = 2K^2 + H + N + 2Q \\
 \epsilon_3 &= K^2 + H + Q \\
 \alpha_6 &= \alpha_5^2 + \epsilon_{d1} = \left(\frac{-1}{2}\right)^2 + K^2 + N + Z + Q \\
 \alpha_6 &= \frac{1}{4} + K^2 + N + Z + Q \\
 \alpha_7 &= 2\alpha_4 \alpha_5 - \epsilon_{d2} = -2K^2 - N - H = 2Q \\
 \alpha_8 &= \alpha_4^2 + \epsilon_3 = K^2 + H + Q \\
 \alpha_9 &= \alpha_3 \alpha_7 + \alpha_5^2 \alpha_8 + \alpha_6 = \frac{1}{4} + Z \\
 \alpha_{10} &= \alpha_1 + 2\alpha_4 \alpha_5 + 2\sqrt{\alpha_8} = 1 + 2\sqrt{K^2 + H + Q} \\
 \alpha_{11} &= \alpha_2 - 2\alpha_5 + 2(\sqrt{\alpha_9} + \alpha_3 \sqrt{\alpha_8}) \\
 \alpha_{11} &= 2 + 2\left(\sqrt{\frac{1}{4} + Z} + \sqrt{K^2 + H + Q}\right) \\
 \alpha_{12} &= 2\alpha_4 \alpha_5 + \sqrt{\alpha_8} = \sqrt{K^2 + H + Q} \\
 \alpha_{13} &= \alpha_5 - (\sqrt{\alpha_9} + \alpha_3 \sqrt{\alpha_8}) \\
 \alpha_{13} &= -1/2 - \left(\sqrt{\frac{1}{4} + Z} + \sqrt{K^2 + H + Q}\right)
 \end{aligned} \tag{26}$$

From the energy spectrum equation, substituting equation (26)

$$n + n^2 - n + n + \frac{1}{2}(2n + 1) \left(\sqrt{\frac{1}{4} + Z} + \sqrt{K^2 + H + Q}\right) - 2K^2 - N - H + 2K^2 - 2H + 2\sqrt{(K^2 + H + Q)\left(\frac{1}{4} + Z\right)} = 0 \tag{27}$$

Making E the subject of the formula

$$E_{n,l} = \frac{-\hbar^2 \alpha^2 \left[\frac{(H-N-Z)}{2(n+\sigma)} + \frac{(n+\sigma)}{2}\right]^2}{2m^*} + \frac{V_0 a}{b} + \frac{\hbar^2 \omega_c^2}{16} \tag{28}$$

$$\text{where } \sigma = \frac{1}{2} + \sqrt{\frac{1}{4} + Z} \tag{29}$$

Results and Discussion

In this study, numerical values were obtained by using the Maple 18 programme code to simulate equations (22), (28) and (29). The input parameters used in this calculation are the effective mass of $\text{Cu}_2\text{ZnSnS}_4$ ($m_{CZTS}^* = 0.208m_0$) where m_0 is free electronic mass, the permittivity of the carrier ϵ is 5.06 (Zongyan and Xiang, 2015), the confining potential constants a and $b = 1$; this is because the number 1 is a unit value, which when assigned to the constants still allows the equation to retain its original physical nature.

Table 1 shows the effect of a varying applied magnetic field B(T) on the energy level E_{nl} of $\text{Cu}_2\text{ZnSnS}_4$ QW with the screening parameter $\alpha = 1$. The choice of B(T) having values from 10–110 is to ensure that the effect of the magnetic field was obvious on the system. The result shows that at the ground state (GS), the first and second excited states (ES) considering the assigned values to the confining potential parameters, the energy level at some points

have values within the range of 1.00–1.50 eV, which corresponds to the results of Liu *et al.* (2015) and Zongyan and Xiang (2015). It is interesting to observe that our simple variational results are in agreement with Liu *et al.* (2015) obtained by using first principles calculation method and of Zongyan and Xiang (2015) obtained by experimental methods. Above the second ES, the energy level becomes inexplicably high and approaches the continuum state. However, at every quantum ES, the energy level shows degeneracy for $\ell = 0$ or 1.

Table 2 shows the relationship between a varying applied magnetic field and the energy level E_{nl} for the screening parameter $\alpha = 2$. Again the energy level at GS, the first and second ES have some values, which correlate with the standard energy band gap as stated by Liu *et al.* (2015) and Zongyan and Xiang (2015). At higher energy levels above the second ES, some of the recorded values are so high (100 eV) that there is currently no physical application for such in the electronic industry because of the unstable nature of

such energy levels but this potential property of CZTS to produce high energy bandgap may be a

good discovery as this may have useful applications as technology advances in electronics.

Table 1: Energy Level for the QW System of $\text{Cu}_2\text{ZnSnS}_4$ with $\alpha = 1, a = 1$ and $b = 1$ under varying External Magnetic Field B(T)

n	ℓ	B(T)	$E_{n,\ell}$ (eV)				
			$V_1 = 0.1$	$V_1 = 0.2$	$V_1 = 0.3$	$V_1 = 0.4$	$V_1 = 0.5$
			$V_1 = 0.6$	$V_1 = 0.7$	$V_1 = 0.8$	$V_1 = 0.9$	$V_1 = 1.0$
0	0	10	0.114176	1.124467	0.026734	1.432133	1.221256
1	0	20	0.712203	0.556789	0.515792	4.201146	0.245002
	1		0.712203	0.556789	0.515792	4.201146	0.245002
2	0	30	0.407801	3.146234	0.515792	3.201236	1.233674
	1		0.407801	3.146234	0.515792	3.201236	1.233674
3	0	40	22.77208	0.024027	0.003211	7.101156	2.105121
	1		22.77208	0.024027	0.003211	7.101156	2.105121
4	0	50	32.16934	32.22011	19.00234	16.00513	2.005144
	1		32.16934	32.22011	19.00234	16.00513	2.005144
5	0	60	84.65600	40.10478	20.34004	30.14221	30.14221
	1		84.65600	40.10478	20.34004	30.14221	30.14221
6	0	70	22.01756	20.60512	45.20101	75.00001	4.100152
	1		22.01756	20.60512	45.20101	75.00001	4.100152
7	0	80	35.54426	46.20011	10.10101	40.65753	56.00127
	1		35.54426	46.20011	10.10101	40.65753	56.00127
8	0	90	38.0021	24.00173	64.30221	107.8778	17.11325
	1		38.00213	24.00173	64.30221	107.8778	17.11325
9	0	100	87.00127	36.11101	84.00126	109.0023	121.0003
	1		87.00127	36.11101	84.00126	109.0023	121.0003
10	0	110	100.2117	44.00443	64.04552	4.120132	4.690434
	1		100.2117	44.00443	64.04552	4.120132	4.690434

Table 2: Energy Level for the QW System of $\text{Cu}_2\text{ZnSnS}_4$ with $\alpha = 2, a = 1$ and $b = 1$ under varying External Magnetic Field B(T)

n	ℓ	B(T)	$E_{n,\ell}$ (eV)				
			$V_1 = 0.1$	$V_1 = 0.2$	$V_1 = 0.3$	$V_1 = 0.4$	$V_1 = 0.5$
			$V_1 = 0.6$	$V_1 = 0.7$	$V_1 = 0.8$	$V_1 = 0.9$	$V_1 = 1.0$
0	0	10	1.114176	2.124467	1.126734	1.414364	1.231256
1	0	20	1.712213	1.016789	1.515792	4.211146	1.245112
	1		1.712213	1.016789	1.515792	4.211146	1.245112
2	0	30	1.417811	3.146234	1.515792	3.211236	1.233671
	1		1.417811	3.146234	1.515792	3.211236	1.233671
3	0	40	22.07218	1.124127	1.113211	7.110156	2.115121
	1		22.07218	1.124127	1.113211	7.110156	2.115121
4	0	50	41.00634	32.22111	19.11234	16.10511	2.115144
	1		41.00634	32.22111	19.11234	16.10511	2.115144
5	0	60	74.75611	41.01478	19.34015	31.14221	31.14221
	1		74.75611	41.01478	19.34015	31.14221	31.14221
6	0	70	22.10756	21.61511	45.20011	75.11111	75.11111
	1		22.10756	21.61511	45.20011	75.11111	75.11111
7	0	80	36.04426	46.21111	0.101111	41.65751	56.11127
	1		36.04426	46.21111	0.101111	41.65751	56.11127
8	0	90	38.11213	24.11172	60.31221	117.8778	17.11325
	1		38.11213	24.11172	60.31221	117.8778	17.11325
9	0	100	70.11127	36.11111	74.10126	119.1123	121.1113
	1		70.11127	36.11111	74.10126	119.1123	121.1113
10	0	110	101.2007	60.10341	88.01552	7.011122	5.601434
	1		101.2007	60.10341	88.01552	7.011122	5.601434

The bandgap energy of the carrier in a CZTS QW is plotted against the cyclotron frequency of the magnetic field B(T) in Figure 1. The plot was for the

GS, the first and second ES (i.e., $n = 0, 1$ & 2). The plot revealed that, at the GS, the cyclotron frequency had no effect on the bandgap energy. At the first ES,

the bandgap energy increased by 0.001 eV and maintained the same energy level showing no change with increasing ω_C .

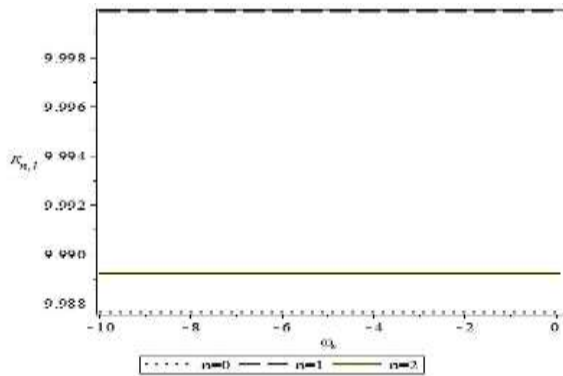


Figure 1: Effect of the Magnetic Field on the Energy Level for the QW System of $\text{Cu}_2\text{ZnSnS}_4$

Figure 2 is a plot showing the relationship between the bandgap energy E_{nl} and the screening parameter α for the GS, first and second ES of the quantum number $n=0,1$ and 2. At the GS, there is little or no effect of the increasing screening on the energy level but at the first and second ES there is a notable increase in the energy level as the screening parameter increases and at the point where $\alpha = 0$, the energy levels of $n = 0, 1$ and 2 converge.

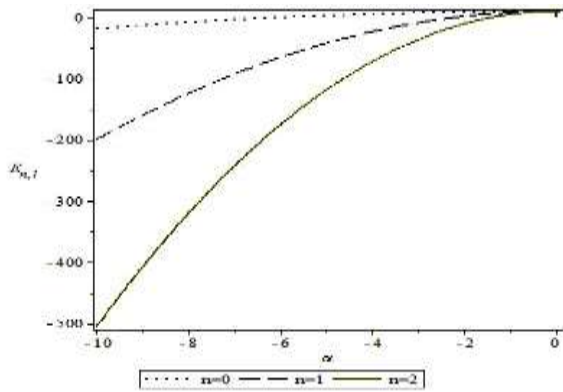


Figure 2: Effect of the Screening Parameters on the Energy Level with Applied Magnetic Fields for the QW System of $\text{Cu}_2\text{ZnSnS}_4$

Figure 3 shows a plot of the effect of potential depth V_0 on the energy level for the GS, first and second ES given by the quantum number $n = 0, 1$ and 2. The plots for these 3 quantum states are interwoven and started from the origin of the graph with the energy level increasing with every increase in V_0 ; suggesting that an increase in the potential depth causes a relative increase in the energy level regardless of the quantum state of $\text{Cu}_2\text{ZnSnS}_4$ QW with an applied magnetic field.

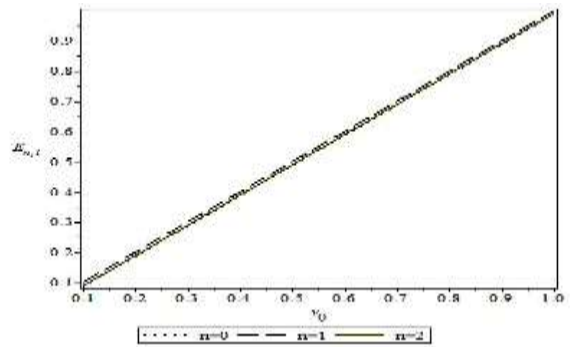


Figure 3: Effect of Potential Depth on the Energy Level with Applied Magnetic Fields for the QW System of $\text{Cu}_2\text{ZnSnS}_4$

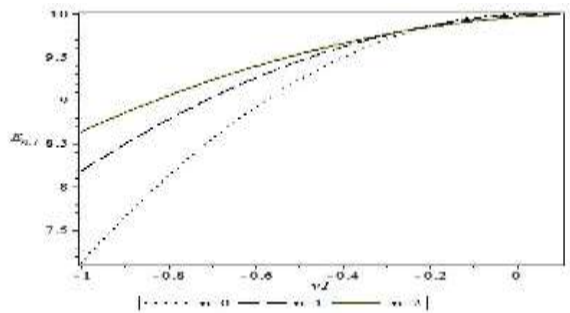


Figure 4: Effect of Potential Depth on the Energy Level with Applied Magnetic Fields for the QW System of Cu_2ZnSnS

Figure 5 reveals the effect of the confining potential parameter V_2 on the energy level E_{nl} for $n = 0, 1$ and 2. A careful observation of the plot shows that at the GS, there is no effect of V_2 on E_{nl} with an applied magnetic field. At the first and second ES, E_{nl} increases by an interval of 0.08 eV for $n = 1$ and an interval of 0.06 eV for $n = 2$ and maintains the same value of E_{nl} for every increase in V_2 . The physical meaning of this is that every quantum state has its own E_{nl} , which is not influenced by changes in V_2 .

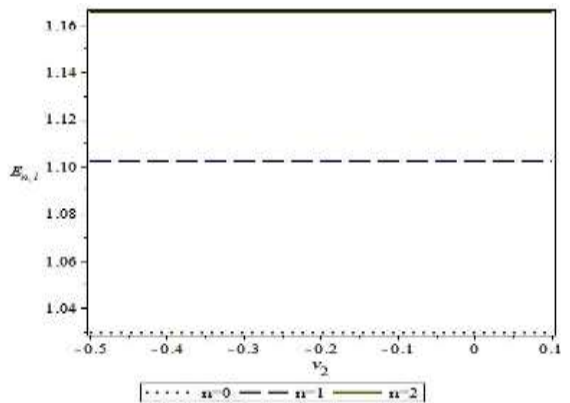


Figure 5: Effect of Potential Parameter on the Energy Level with Applied Magnetic Fields for the QW System of $\text{Cu}_2\text{ZnSnS}_4$

The bandgap energy E_{nl} obtained in this work, which corresponds to reported standard values, were obtained at certain specifications of α , ω_c , V_1 , V_2 , V_0 and n . It can, therefore, be concluded from the results obtained in Tables 1–2, that the magnetic field $B(T)$ can be used as an adjustment measure to obtain the required value of E_{nl} for technological applications. Also, judging from the plots in Figures 1–5, it can be said that the n , V_0 , α , V_1 and V_2 have effects on the bandgap energy E_{nl} .

References

- Allouche, N. K., Nasr, T. B., Kamoun, N. T., Guash, C., (2010). Synthesis and properties of chemical bath deposited ZnS multilayer films. *Materials Chemistry and Physics* **123**: 620–624.
- Aytekin, T., Li, J., Du, H., Yarbrough, J. (2012). Current-voltage characteristics of organic heterostructure devices with insulating spacer layers. *Org Electron.* **24**(21): DOI: 10.1016/j.orgel.201.05.018.
- Bilal, K., Levchenko, S., Gurieva, G., Guc, M. (2014). Nonlinear optical properties of a two-dimensional elliptic quantum dot. *Phys. E* **42**(21): 1477.
- Boda, T. E., Setrap, K. T., Clotterjee, S. E. (2013). Electronic states and interband light absorption in semi-spherical quantum dot under the influence of strong magnetic field. *Solid State Commun.* **13**(10): 537.
- Chen, I., Zhang, Y., Yuan, X., Sun, X. (2013). Linear and nonlinear intra-conduction band optical absorption in (In,Ga)N/GaN spherical QD under hydrostatic pressure. *Opt. Commun.* **31**(21): 73.
- Greene, R. L., Aldrich, C. (1976). Variational wave functions for a screened coulomb potential. *Physical Review A*, **14**(6): 2363–2366
- Hassanabadi, H., Ikot, A. N., Onyenegecha, C. P., (2017). Approximate bound and scattering solutions of Dirac equations for the modified deformed Hylleraas potential with a Yukawa-type tensor interaction. *Indian Journal of Physics*, **54**(6): 74–83.
- Ikot, A. N., Oladunjoye, A. A., Akaninyene, D. A., (2013). Bound state solution of D-dimensional Schrodinger equation with Eckart potential plus modified deformed Hylleraas potential. *Chinese Physics B*, **22**(2): 83–94.
- Karasslan, W., Hall, S. R., Szymanski, J. T., Stewart, J. M. (2016). Nonlinear optical properties of a hydrogenic impurity in an ellipsoidal finite potential quantum dot. *Curr. Appl. Phys.*, **11**(2): 176.
- Liu, H., Embreus, O., Stahl, A., Dubois, T., Papp, G., (2015). Optical properties of excitonic polarons in semiconductor quantum dots. *Phys. E*, **21**(20): 164–168.
- Panahi, H., Golshahi, S., Doostdar, M. (2013). Influence of position dependent effective mass on donor binding energy in square and V-shaped quantum wells in the presence of a magnetic field. *Physica B*, **418**(20): 47–51.
- Pena, J. J., Ovando G., Morales, J. (2015). D-dimensional Eckart deformed Hylleraas potential bound state solutions. *Journal of Physics: Conference series* **574**(1): 012089.
- Uplane, M. D., Kshisagan, P. N., Lokhande, B. J., Bhosale, C. H. (2000). Properties of transparent conducting sulphides. *Materials in Chemistry and Physics*, **64**(3): 75.
- Wang, W., Winkler, M. T., Gunawan, O., Gokmen, T., Todorov, T. K., Zhu, Y., Mitzi, D. B. (2013). "A 12.6% $\text{Cu}_2\text{ZnSnSxSe}_{4-x}$ (CZTSSe) solar cell is presented with detailed device characteristics". *Advanced Materials*, **17**(3): 213–217.
- Zongyan, Z., Xiang, Z. (2015). Electronic, optical and mechanical properties of $\text{Cu}_2\text{ZnSnS}_4$ with four crystal structures. *Journal of Semiconductors*, **36**(8): 45–49.